Report 3647

LOCATION OF SEPARATION ON A CIRCULAR CYLINDER IN
CROSSFLOW AS A FUNCTION OF REYNOLDS NUMBER

NAVAL SHIP RESEARCH AND DEVELOPMENT CENTER

Bethesda, Maryland 20034

[redacted]

LOCATION OF SEPARATION ON A CIRCULAR CYLINDER IN CROSSFLOW AS A FUNCTION OF REYNOLDS NUMBER

by

David W. Coder

APPROVED FOR PUBLIC RELEASE: DISTRIBUTION UNLIMITED

SHIP PERFORMANCE DEPARTMENT

RESEARCH AND DEVELOPMENT REPORT

November 1971 Report 3647

The Naval Ship Research and Development Center is a U. S. Navy center for laboratory effort directed at achieving improved sea and air vehicles. It was formed in March 1967 by merging the David Taylor Model Basin at Carderock, Maryland with the Marine Engineering Laboratory at Annapolis, Maryland. The Mine Defense Laboratory (now Naval Ship R & D Laboratory) Panama City, Florida became part of the Center in November 1967.

Naval Ship Research and Development Center

Bethesda, Md. 20034

MAJOR NSRDC ORGANIZATIONAL COMPONENTS

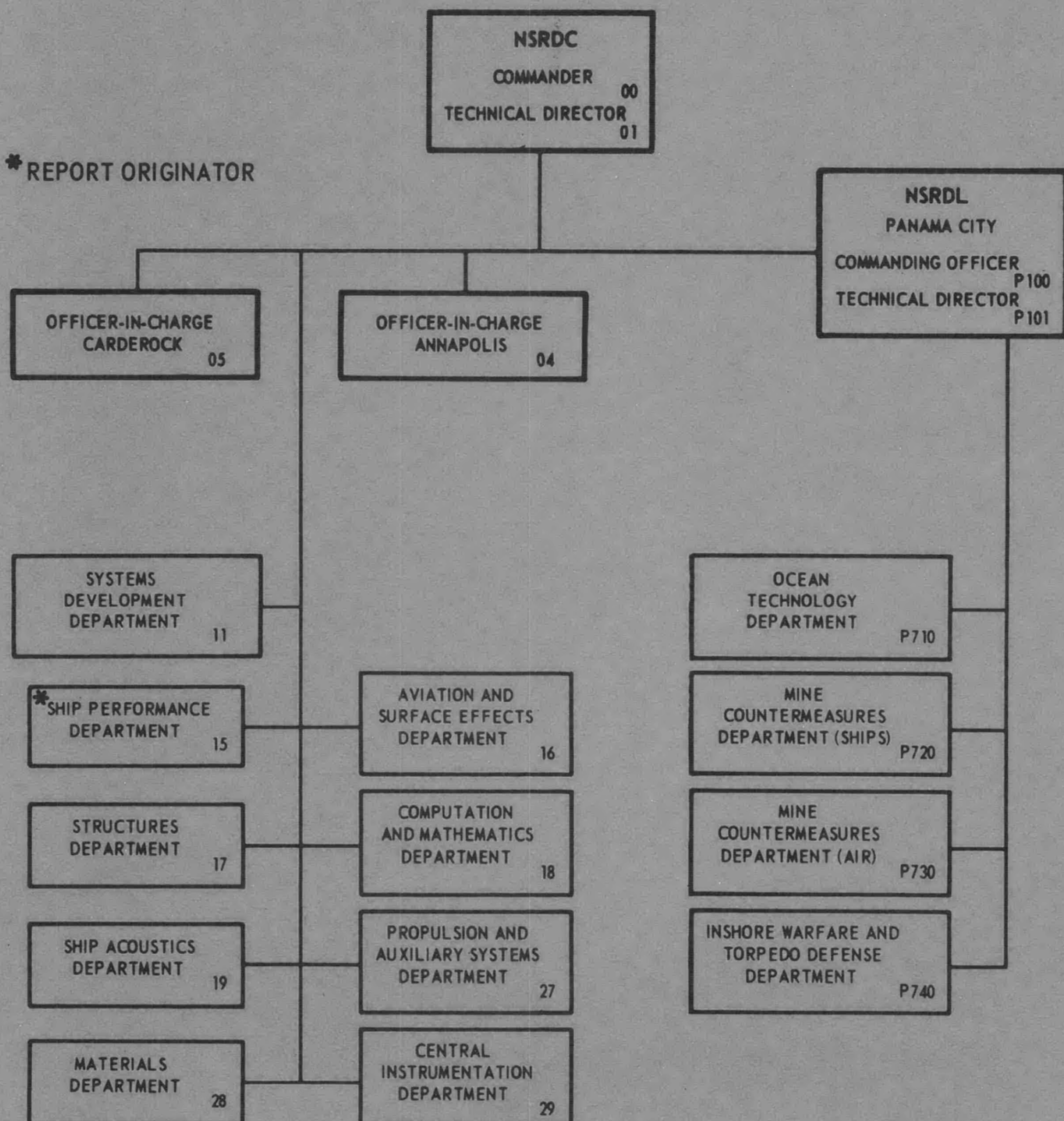

NDW-NSRDC 3960/43 (3-70)
NDW-NSRDC 3960/44 (REV. 8/71)

GPO 917-872

DEPARTMENT OF THE NAVY
NAVAL SHIP RESEARCH AND DEVELOPMENT CENTER
BETHESDA, MD. 20034

LOCATION OF SEPARATION ON A CIRCULAR CYLINDER IN CROSSFLOW AS A FUNCTION OF REYNOLDS NUMBER

by

David W. Coder

APPROVED FOR PUBLIC RELEASE: DISTRIBUTION UNLIMITED

November 1971

Report 3647

TABLE OF CONTENTS

LIST OF FIGURES

LIST OF TABLES

NOTATION

c	Speed of sound in media
D	Diameter of cylinder
H3, H5	Hot film gages located on port side of cylinder
H10, H11	Hot film gages located on starboard side of cylinder
M	Mach number = U_∞/c
p	Local pressure
R_n	Reynolds number = $U_\infty D/\nu$
r	Distance from center of cylinder
U	Local potential velocity
U_∞	Free stream velocity
$U_\infty\uparrow$	Slowly accelerating free stream velocity
$U_\infty\downarrow$	Slowly decelerating free stream velocity
X	Nondimensional distance (distance divided by diameter) around the surface of the cylinder from the forward stagnation point
Θ	Angle from forward stagnation point of cylinder
ν	Kinematic viscosity
ρ	Density
ϕ_s	Separation angle from forward stagnation point

ABSTRACT

All available information on the location of separation on a circular cylinder in crossflow as a function of Reynolds number (from "creeping" flow to "transcritical" flow) has been summarized. The results of an experiment by the author in the "transition" (or "supercritical") flow regime are included. The various theoretical and experimental results are discussed and compared. Areas needing additional theoretical and experimental work are pointed out.

ADMINISTRATIVE INFORMATION

The experiments by the author were sponsored by the Naval Ship Systems Command Subproject S4611 010, Task 11098. This report was prepared under the support of the Naval Ship Research and Development Center (NSRDC) Training Program.

INTRODUCTION

A literature survey on the incompressible, viscous flow around a right circular cylinder reveals that experimental information on the location of flow separation is sparse and not well organized. One prominent investigator feels that it would be both valuable and fairly easy to measure the position of separation as a function of Reynolds number over the whole shedding range.[1]

There is, however, much experimental data on the average pressure distribution around a cylinder from which separation information may be obtained. These data, other experimental and theoretical data from the literature, and the results of an NSRDC experiment treat separation angle as a function of Reynolds number, from a very small Reynolds number to the transcritical flow regime. Reynolds number ranges that need additional experimental and theoretical information are pointed out in the report.

---

[1]References are listed on page 22.

EXPERIMENTAL RESULTS

RESULTS FROM EXISTING LITERATURE

Three different approaches have been used to determine experimentally the angle of separation on a circular cylinder in crossflow. Many investigators[2-13] have determined the average pressure distribution on the surface of a cylinder. From these distributions the approximate average separation angle was determined by noting the inflection point aft of the first minimum pressure point. These data are presented in Table 1. According to Goldstein[14] (see pp. 421-427), this inflection point in the pressure distribution coincides with a minimum in shear stress on the surface which indicates the boundary layer has separated from the surface. The maximum possible error in determining inflection points by this method depends on how clearly defined the points are. The range of confidence that this author has in his determination of the points is as much as ±5 deg in some cases and less than ±1 deg for others. For completeness, this range of confidence in each reading is included in the tables and figures.

A few values for the separation angle have been determined by flow visualization using dye in water.[15,16] These results are also listed in Table 1. More accurate measurements (also listed in Table 1) have been made by determining the minimum shear point (or points) on the cylinder aft of the front stagnation point either by a surface tube[3,17] or by hot films.[18] The latter method provides data on the separation angle accurate to within ±1 deg. It is felt that this is the easiest and most accurate method for determining separation angles. This method was also used by the author for the experimental work discussed in the next section.

EXPERIMENTS PERFORMED BY THE AUTHOR

The high speed basin and Carriage 5 at NSRDC were used for the experiments. The pitch-heave oscillator[19] mounted on Carriage 5 was used to support a smooth circular cylinder, 1 ft in diameter and 6 ft long, horizontally at a depth of 4 ft. The two large struts that supported each end of the cylinder were flat on the inside to ensure two-dimensional flow across most of the cylinder. While the carriage was moving, the pitch-heave oscillator was capable of slowly rotating the cylinder 6 deg down and

10 deg up from its zero position. From the Cahn data,[18] all separation angles would be between 75 and 85 deg for Reynolds numbers between 3×10^4 and 3×10^5, where Reynolds number is defined as free stream velocity times the diameter over the kinematic viscosity. Hot film gages were placed spanwise along the cylinder at an angle of 78 deg to allow movement of the gages from 72 to 88 deg to sufficiently cover the separation angles reported by Cahn.[18]

The type of hot film anemometer used on the test was the end-mounted cylindrical type obtained from Lintronic Lab, Silver Spring, Maryland. The gage is basically two thin wires set parallel along the axis in a glass cylinder with a thin platinum wire mounted on the end of the cylinder across the ends of the two wires. This glass cylinder was then mounted in the end of a stainless steel tube 0.095 in. in diameter and 1 1/8 in. long. The gages were mounted in the test cylinder with the end of the gage flush with the surface of the cylinder. The gage subtended an angle of less than 1 deg of the surface of the test cylinder. The gage resistance was between 10 and 15 ohm. A resistor of about 85 to 90 ohm was connected in series with the gage to form the active arm of a 100 ohm bridge. The bridge was powered and balanced by an ENDEVCO constant current signal conditioning unit.

The gages operate on the principle of a change in resistance due to temperature change. The heat transfer of the I^2R heat generation in the gage is mostly transferred to the water. This heat transfer process to the water is very much dependent upon the flow over the hot film. Thus, as the flow changes, the heat transfer changes, changing the operating temperature of the gage. The changes in resistance due to the temperature change result is a resistance imbalance in the bridge which changes the voltage output.

A rough calibration of the gages was done by inserting them into a pipe in which water was being displaced by a piston. The results showed that some of the gages were as much as twice as sensitive as others. However, this fact caused no difficulty since it had been planned to use these gages for qualitative data only.

The steel test cylinder had a 6-in. long aluminum test section in the middle. The test section was separated from the rest of the cylinder by less than 0.015 in. on the port side and 0.007 in. on the starboard side. These slight discontinuities and the slightly different surface (aluminum instead of steel) seemed to somewhat isolate the two sides of the test cylinder for some of the results. Gages H3 and H5 were located 18 and 12 in. from the center of the test cylinder on the port side and Gages H10 and H11 were located 15 and 19 in. from the center of the starboard side. Other gages were mounted on the cylinder also, but only these four were operational for the whole test. Thus, data from only these four gages is presented here.

Experiments were first conducted in a manner similar to Reference 18, i.e., first establishing a steady carriage velocity and then rotating the cylinder slowly so that the gages would be rotated from 72 to 88 deg. It was found that the method was unsuited for carriage operation (although not for wind tunnel operation) since the run time was limited by the length of the basin, especially for higher velocities. It was suggested by Mr. H. D. Harper of the staff that a more appropriate method would be to hold the angle fixed and vary the velocity. Significant changes in the flow pattern for the fixed geometry would then be easily detected. This turned out to be a much easier method. As the velocity was slowly increased or decreased, the velocity at which the separation point passed by the gage could be easily determined. Figure 1 shows a case when the velocity was increased so that the gages were first in the wake, showing oscillating eddies, and then in the stream ahead of the wake. Results for separation angle versus Reynolds numbers for this method are listed in Table 2 and shown in Figure 2. An interesting result is the obvious difference in the separation velocity for the given angle depending on whether the flow is slowly accelerating or decelerating. The separation velocity appears to be about a tenth of a knot lower for decelerating flow than for accelerating flow. Also the amount of scatter in the accelerating flow data is much greater. A general result of the data is that separation angle increases significantly with Reynolds number in the Reynolds number range from about 2×10^5 to 3×10^5.

SUMMARY

Data listed in Table 2 for slowly decelerating flow for Gage H10 is combined with all of the data listed in Table 1 and shown in graphical form in Figure 3. From this graph, together with discussions from the various references listed in Table 1, some general trends may be established. For very small Reynolds numbers (below about 5-10) the flow is symmetrical around the cylinder with no separation. Separation begins near the rear stagnation point at a Reynolds number of about 5-10. Two small vortices occur symmetrically in the separated region. As the Reynolds number is increased these vortices grow but remain symmetrical to the stagnation streamline and the separation point moves toward the front of the cylinder as shown in Figure 3. At a Reynolds number of about 40, the vortices start to be shed from the cylinder in an asymmetrical pattern. Thus, the separation angle oscillates around the cylinder as the vortices are shed alternately from one side to the other. The average separation angle only is considered in Figure 3. It seems as though the average separation angle changes significantly whenever the vortices have begun to shed. Figure 3 shows a jump of about 30 deg in separation angle near a Reynolds number of 40. However, since this trend is observed from just a few data points, more data should be taken in this Reynolds number range to determine if there is any continuous transition. Up to Reynolds numbers of about 150-300, the boundary layer and the shed vortices are laminar. Above this Reynolds number the boundary layer remains laminar but the separated flow becomes turbulent.

As seen in Figure 3, there seems to be little effect on the separation angle due to separated flow becoming turbulent. This laminar separation with turbulent vortices persists until the critical Reynolds number (somewhere between 3×10^4 and 3×10^5) is reached. The regime of flow below this Reynolds number is known as the subcritical regime. In this regime, the separation angle continually decreases with increasing Reynolds number as shown in Figure 3. It appears that at a Reynolds number of 10^3 to 10^4 the separation angle has reached 90 deg, or the point of maximum thickness of the cylinder.

The "critical" Reynolds number, which marks the beginning of the transition or supercritical regimes, is somewhere between 3×10^4 and 3×10^5 depending on surface roughness, turbulence in the free stream, and vibrations of the cylinder. In this regime the separation angle changes from less than 90 deg to larger than 90 deg. However, due to the differences of "critical" Reynolds number because of different experimental setups and techniques, the relationship between separation angle and Reynolds number is obscured in Figure 3. Replotting some selected transition regime data that seem to have approximately the same beginning point ("critical" Reynolds number), one may clearly see the effect during transition. This has been done in Figure 4 for data from References 6, 18, and the present data. The data indicate a continuous decrease in separation angle with increasing Reynolds number in the transition regime. Just before the transcritical regime, which begins somewhere between $R_n = 10^6$ and 3.5×10^6, a rapid but *continuous* increase in the separation angle is seem. The angle increases to above 90 deg but below about 100 deg.

In the Reynolds number range between 10^5 and 10^6, laminar separation occurs, but the turbulent separated flow reattaches to the cylinder and finally turbulent separation occurs. In this regime two separation angles may be found. The laminar separation occurs between 90-100 deg and the final turbulent separation between about 125-145 deg as shown in Figure 3.

In the transcritical regime (Reynolds numbers greater than about 10^6), the boundary layer becomes turbulent before separation. In this regime the separation angle appears to move forward again with increasing Reynolds number to about 100 deg at a Reynolds number of 10^7 as shown in Figure 3.

THEORETICAL RESULTS

The viscous flow past a circular cylinder has been solved for small Reynolds numbers (see Article 343, Reference 20). For small Reynolds numbers, the inertia forces are small with respect to the viscous forces. The method of solution is to approximate the Navier-Stokes equations by either neglecting inertia terms or taking them partially into account after the manner of Oseen. The former method is considered a good approximation for $R_n < 1$ and the latter is considered good up to about $R_n = 5$ (Reference 21). The results of these methods yield a symmetrical wake with no separation.

For larger Reynolds numbers the inertia terms must be retained and the Navier-Stokes equations are either solved using "boundary layer theory" or a numerical integration of the full Navier-Stokes equations.

LAMINAR BOUNDARY LAYER METHODS

From boundary layer theory, the flow field about a solid boundary is divided into that of a thin layer next to the body surface where viscous forces are very important and that away from the surface for which the viscous forces are not as important and may be neglected. In the former area, the simplified Navier-Stokes equations, known as "Prandtl boundary layer equations" are used to describe the flow. These equations are derived by assuming a very large Reynolds number and a very thin boundary layer thickness with respect to body dimensions. It turns out that the pressure across the boundary layer remains practically constant. The method of solution requires that the pressure along the boundary layer be known. Since the boundary layer is very thin, the pressure at the outer edge of the boundary layer may be calculated using potential theory. Also experimental data may be used for the pressure distribution. The point of separation is then defined as the point at which the velocity gradient normal to the surface becomes zero. This is also the point for zero shear on the surface.

The velocity distribution around a circular cylinder from potential flow may be written in terms of X, the nondimensional distance along the surface of the cylinder from the forward stagnation point.

$$U(X) = 2\ U_{\infty} \sin X$$

This velocity distribution may be expanded in a power series (referred to as a Blasius Series) in terms of X. Using Bernoulli's equation, the pressure gradient along the boundary layer is found to be

$$\frac{dp}{dX} = -\rho U \frac{dU}{dX}$$

where ρ is density.

From the boundary layer equations and a step-by-step iterative procedure from the front stagnation point, the separation angle is found to be 108.8 deg and 109.6 deg from the forward stagnation point for the Blasius series including terms up to X^7 and X^9, respectively.[22] By comparing these values for separation angle with the experimental results, it is seen that the Blasius results are too low for the symmetric vortices regime ($3.5 \leq R_n \leq 40$) and much too high for subcritical Reynolds numbers above 40 where there are asymmetric vortices. In reality the pressure distribution for these Reynolds numbers is much different from the potential flow distribution. The transcritical pressure distribution is much closer to the potential distribution so that one would expect a better agreement with transcritical flow. This is seen to be the case as shown in Figure 5.

Hiemenz[2] experimentally measured the pressure distribution for a given Reynolds number and assumed a Blasius series of three terms in powers of X to represent this distribution. The separation angle using this distribution is found to be 82 deg from the calculations compared with his experimental measurement of 81 deg. This semi-empirical method is a considerable improvement over the original Blasius solution. Whereas the Blasius solution indicates that the separation angle is greater than 90 deg, or aft of the maximum thickness section of the cylinder, for any Reynolds number, the Hiemenz solution indicates angles of less than 90 deg for the particular Reynolds number of 1.85×10^4. It is seen in Figure 5 that this result is much more realistic for subcritical flow. Refinements of the Hiemenz solution have been made by other authors[23-29] and have been summarized by Cahn.[18] The results, in general, give slightly smaller values for the separation angle than did the Hiemenz solution for the same conditions. Smith and Clutter[27] found a separation angle of 80.0 deg and Curl and Skan[26] about 78 deg for the particular Reynolds number of 1.85×10^4.

Howarth[30] repeated the Hiemenz calculations for the pressure distribution in transition flow regime at a Reynolds number of 2.12×10^5 measured by Fage and Faulkner[3] and at a Reynolds number of 6.7×10^5 measured by Flachsbart.[4] The results were 116 deg for the former and 117 deg for the latter. These results are seen to be more reasonably expected for transcritical flow than for the transition regime.

An approximate solution based on the Blasius method was developed by Pohlhausen[31] to simplify the calculations. The separation angle for a potential velocity distribution was found to be 109.5 deg compared with the exact value of 108.8 deg calculated by Blasius. Using the Hiemenz experimental pressure distribution, Pohlhausen found the separation angle to be 81.5 deg compared with a Hiemenz value of 82 deg. A more detailed review of these methods may be found in Chapter 9 of Reference 14 and Chapters 9 and 12 of Reference 21.

Ujihara[32] has used the experimental results from the boundary layer region together with the boundary layer equations to develop a semi-empirical "Generalized Kutta Condition." This condition determines the time rate of vorticity transport from the shear layer region, and the locations on the surface from which this vorticity is released. Using this information he considers the flow around the cylinder potential flow and feeds in the appropriate vorticity in order to examine how this vorticity is distributed in the wake area. The circular cylinder is represented by a source-sink doublet in uniform flow. Vorticity is fed into the flow field at the first pressure minimum aft of the forward stagnation point on both sides of the cylinder. The magnitude of the vorticity transport is equal to half the square of the local tangential velocity at the feeding points. The normal flow at the surface from each discrete vortex fed into the flow is nulled by an image vortex inside the cylinder. A numerical solution is obtained by finite difference in time. The initial flow conditions are considered to be that for steady potential flow around a cylinder in a uniform stream with some small initial asymmetry to perturb the flow symmetry. After a steady flow condition is reached, the average pressure distribution is obtained. From this distribution the separation angle is found to be 90 ± 5 deg for a Reynolds number of 200. This value agrees well with the experimental results shown in Figure 5.

NUMERICAL SOLUTION OF THE NAVIER-STOKES EQUATIONS

Numerical solutions of the viscous flow around a circular cylinder have been obtained for discrete Reynolds numbers. Thom[5] and Kawaguti[33] have obtained steady solutions and Payne,[34] Trulio et al,[35] and Thoman and Szewczyk[36] have obtained unsteady solutions.

Thom[5] considered the flow over the upper half of a circular cylinder for a Reynolds number of 20. Thus, the resulting solution is for flow symmetrical to the zero streamline. This symmetry is reasonable for Reynolds numbers below about 40 where the flow has been shown by experiments to be symmetrical. Above this Reynolds number alternate shedding of vortices occur and the whole flow field must be considered. The Thom grid was a network of potential flow streamlines and equipotential lines. He applied numerical techniques to the steady vorticity transport equations (a form of the Navier-Stokes equations) in which the stream function and vorticity are the independent variables. He initially assumed values for these variables at each corner of the grid quadrilaterals and evaluated the values at the centers of each quadrilateral. He then found new values at the corners. Repeating this procedure over and over, the field eventually converged. He then determined an average pressure distribution from which this author determined the separation angle to be about 122 deg by noting the inflection point. It is seen in Figure 5 that this value agrees well with symmetrical experimental values. Kawaguti[33] obtained a solution for symmetrical, steady flow around a circular cylinder at a Reynolds number of 40. The Kawaguti grid was comprised of Θ-constant lines and 1/r-constant lines. Using a numerical representation of the steady vorticity transport equation, he proceeded from assumed initial values for vorticity and stream function using a method similar to Thom[5] until the flow parameters converged. For a Reynolds number of 40, he found a separation angle (zero vorticity on the surface of the cylinder) of 127.8 deg. This value of separation agrees well for the symmetrical experimental results shown in Figure 5.

Payne[34] obtained a time-dependent solution for the flow around the upper half of a circular cylinder (i.e., symmetric case) for Reynolds numbers of 40 and 100. He numerically integrated the vorticity transport equation using central difference formulae for the space derivatives and a forward difference formula for the time derivatives. The mesh was comprised of Θ-constant lines and log r-constant lines. The flow was impulsively started at time equal to zero. For a time of 6 (unit time being the time necessary for the fluid at infinity to move a distance equal to the radius of the cylinder) the separation angles (zero streamlines) were found to be 140 deg and 134 deg for Reynolds numbers of 40 and 100, respectively. These results appear to be too high to be realistic.

Trulio et al[35] obtained the time-dependent compressible flow around a circular cylinder for discrete Reynolds numbers from 100 to 5000 and a Mach number of 0.2. They considered both symmetric and alternating shedding cases. The Navier-Stokes equations were used to govern the flow of the fluid and a polytropic gas equation of state was used for the fluid pressure. Three different fixed grids were used. The meshes were comprised of quadrilaterals that were rectangular away from the cylinder and similar to potential flow streamlines and equipotential lines near the cylinder. A finite difference scheme was chosen that ensured conservation of total energy of the system. The exact scheme is not reported but earlier work by the authors is referenced. The initial conditions were impulsive and in the asymmetric case, the flow was perturbed by slightly flattening the cylinder on the top. Most of the data presented in the report are graphic representations of the flow field using small arrows to depict the magnitude and direction of the velocity. Only the fine grid yields good information on the near wake. Using this grid, one symmetric study was reported for a Reynolds number of 10^3. For this case a separation angle of 108 ± 2 deg may be determined. The flow field, however, has not yet come to a steady rate. The time from the initial impulsive flow is equivalent to the time necessary for a free stream particle to move 1.25 cylinder diameters. Using the medium grid, only a very rough approximation of 122 ± 5 deg may be made for the separation angle for alternate shedding for a Reynolds number of 10^2. A free stream particle has traveled 17.1 diameters for this case.

Thoman and Szewczyk[36] obtained the alternate vortex shedding flow around a circular cylinder for discrete Reynolds numbers from 1 to 10^6 using finite difference techniques on the vorticity transport equations. The grids were comprised of potential flow streamlines and equipotential lines. Two different size grids were used. The flow was impulsively started and the separation angle was determined after several time steps (enough to obtain steady periodic results) by detecting the location of minimum shear on the surface of the cylinder aft of the forward stagnation point. The separation angles for Reynolds numbers of 30, 200, 4×10^4, and 3×10^5 were found to be 134 deg, 116 deg, 84 deg, and 80 deg, respectively.

In general, Figure 5 shows that the separation angles determined by integrating the unsteady Navier-Stokes equations (Payne,[34] Trulio,[35] Thoman and Szewczyk[36]) agree with the symmetric experimental values below a Reynolds number of about 40 (except for Payne[34] which are too high), but are much higher for Reynolds numbers between 40 and about 10^4. Above about 10^4 the results concur with the lower bound of the experimental results for the subcritical regime.

SUMMARY

Both for simplicity and accuracy, hot films is the best technique available to determine the location of separation on a circular cylinder. In the subcritical and transition regimes of flow the technique is far superior, and it should be no worse than other techniques in the transcritical regime. The limited circumferential range of the hot films reported here gave separation results for only a limited Reynolds number range. It would be well to repeat the experiment with more circumferential range to increase the range of Reynolds numbers. It would be well to conduct experiments in all ranges of Reynolds numbers using this technique to supplement data in this report.

The new data presented in this report show that in the transition regime just before the transcritical, there is a rapid but continuous increase in the separation angle. The separation angle also demonstrates a hysteresis characteristic. As the Reynolds number (velocity) is slowly increased, the separation angle increases. However, if the Reynolds number is slowly decreased, the separation angle does not increase until the Reynolds is reduced about 10 percent. It is not known whether this hysteresis effect occurs in other Reynolds number ranges.

More experimental work is needed for Reynolds numbers around 40 to determine whether there is a continuous transition from two fixed vortices to alternate shedding, or whether the separation angle "jumps" 30 deg.

For Reynolds numbers below about 40 where the vortices behind the cylinder are either symmetric or nonexistent, the results for separation angle obtained from the steady Navier-Stokes equations (see Thom[5] and Kawaguti[33]) give good agreement with experimental results.

For a Reynolds number of 200, the semi-empirical theory of Ujihara[32] agrees well with experimental results. This is the only theoretical result that agrees with experimental results in the subcritical regime for $40 < R_n < 10^4$. This type of solution should be attempted at other Reynolds numbers, say 10^2, 10^3, and 10^4, if practical. Solutions in the Reynolds number range using the unsteady Navier-Stokes equations (Payne,[34] Trulio,[35] Thoman and Szewczyk[36]) give larger separation angles than experiments indicate.

In the subcritical regime for $R_n > 10^4$, the solutions using the unsteady Navier-Stokes equations agree well with experiments. Also, the Hiemenz[2] solution using the experimental pressure distribution in the Blasius theory[22] yields good results for $R_e = 1.85 \times 10^4$. This semi-empirical technique should be tried for smaller Reynolds numbers in the subcritical regime.

The Hiemenz-type solutions have been tried by Howarth[30] for the transition regime. The results are extremely high; they agree better with the experimental results for the transcritical regime.

ACKNOWLEDGMENTS

The author gratefully acknowledges the assistance of Messrs. W. G. Souders and H. D. Harper in conducting the experiments.

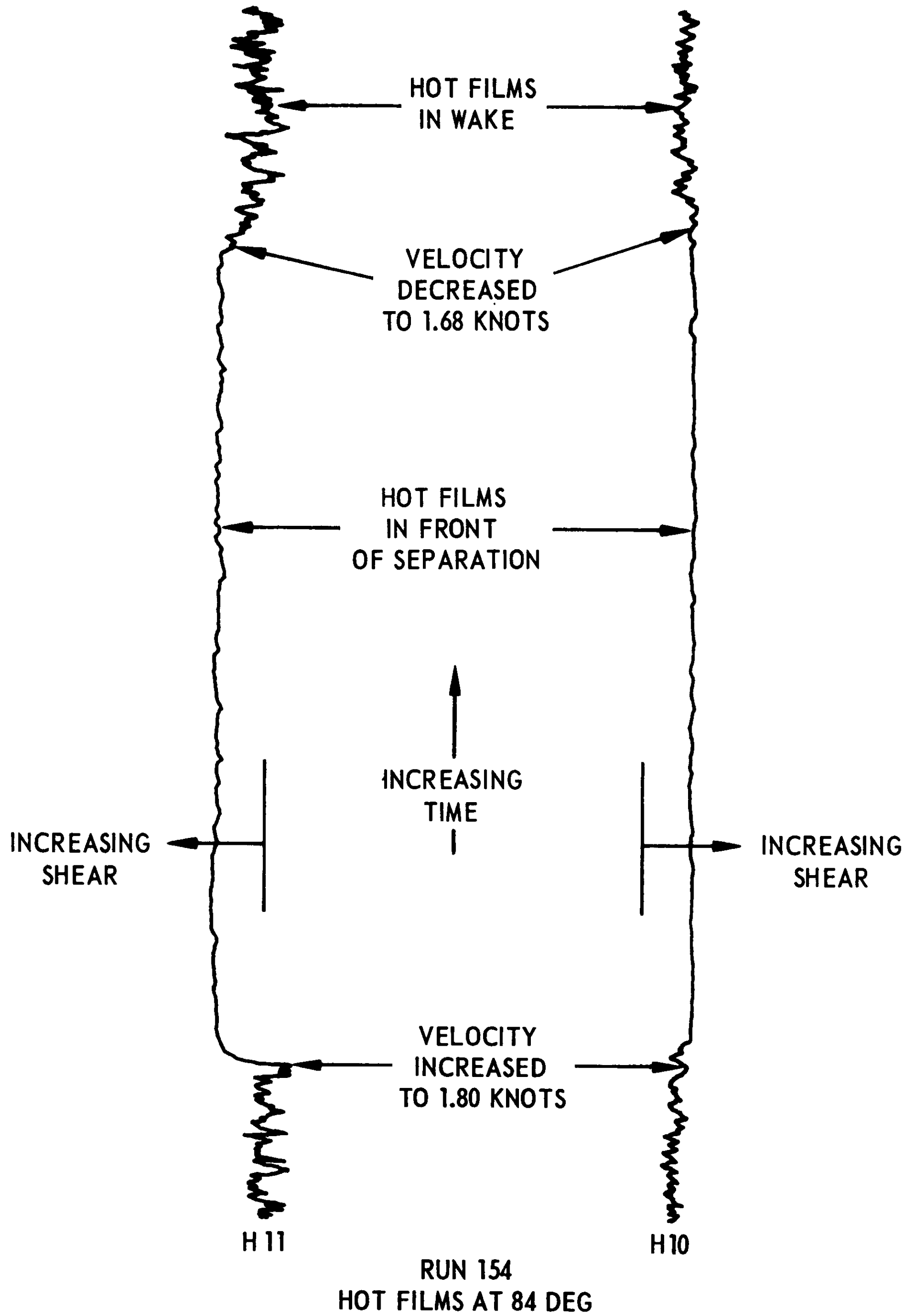

Figure 1 - Sanborn Record Showing Hot Film Outputs as Separation Point Moves around the Cylinder

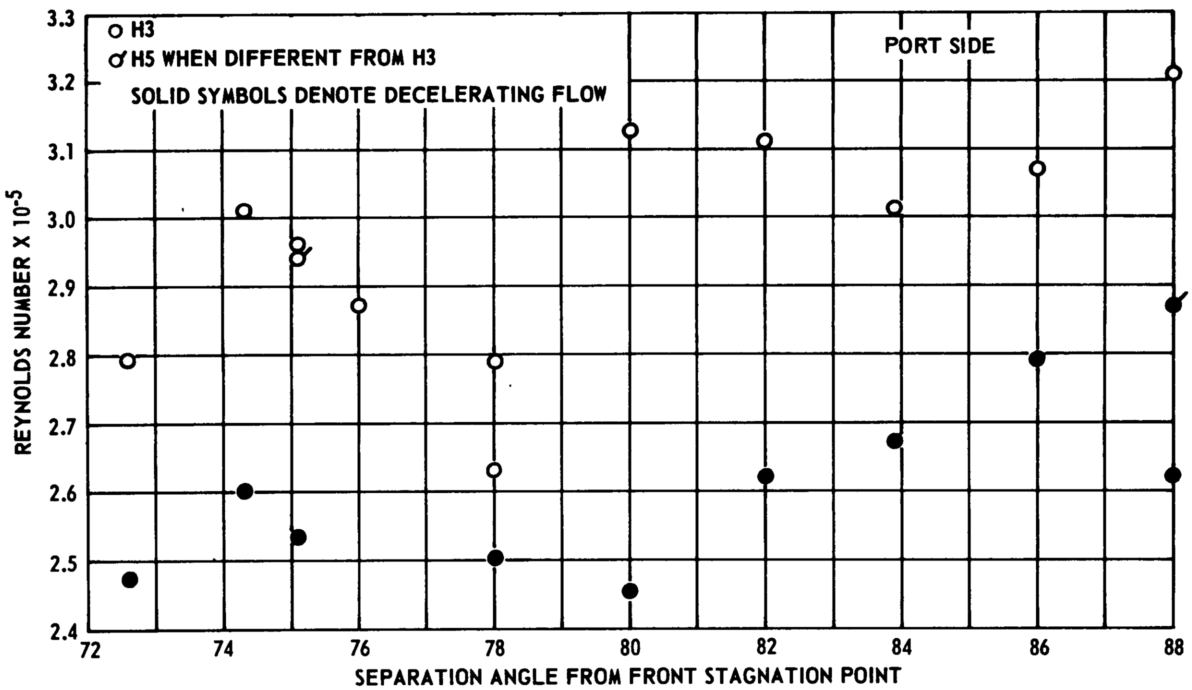

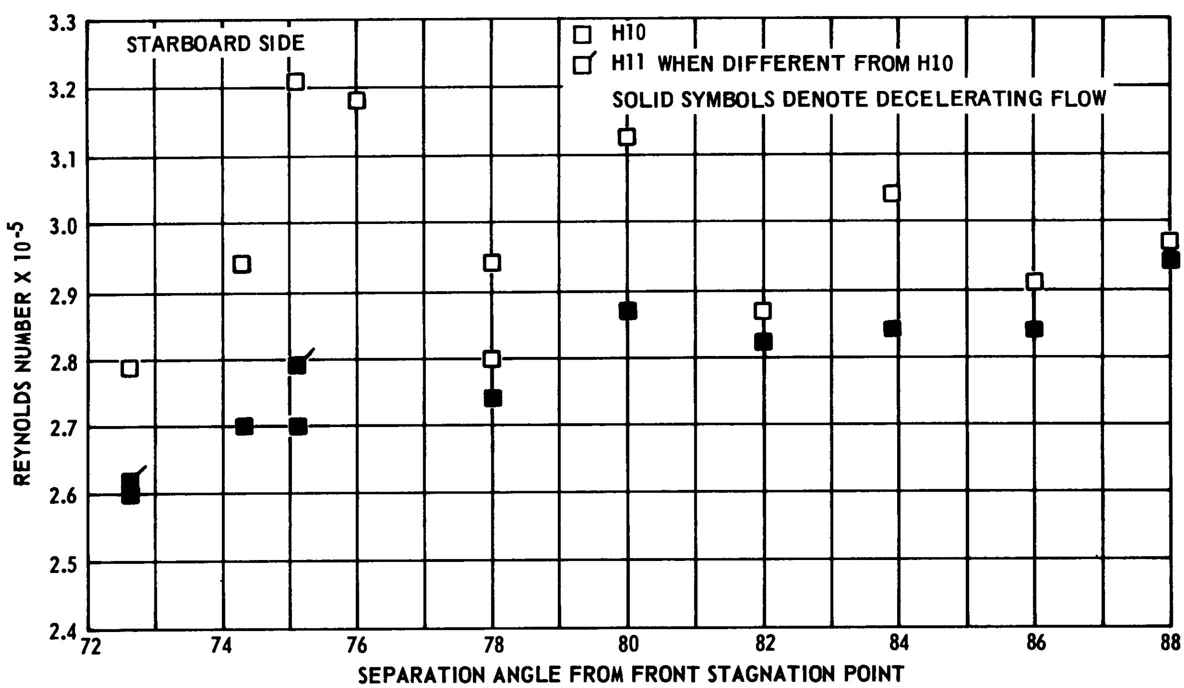

Figure 2 - Separation Angle versus Reynolds Number for Experiments by Author

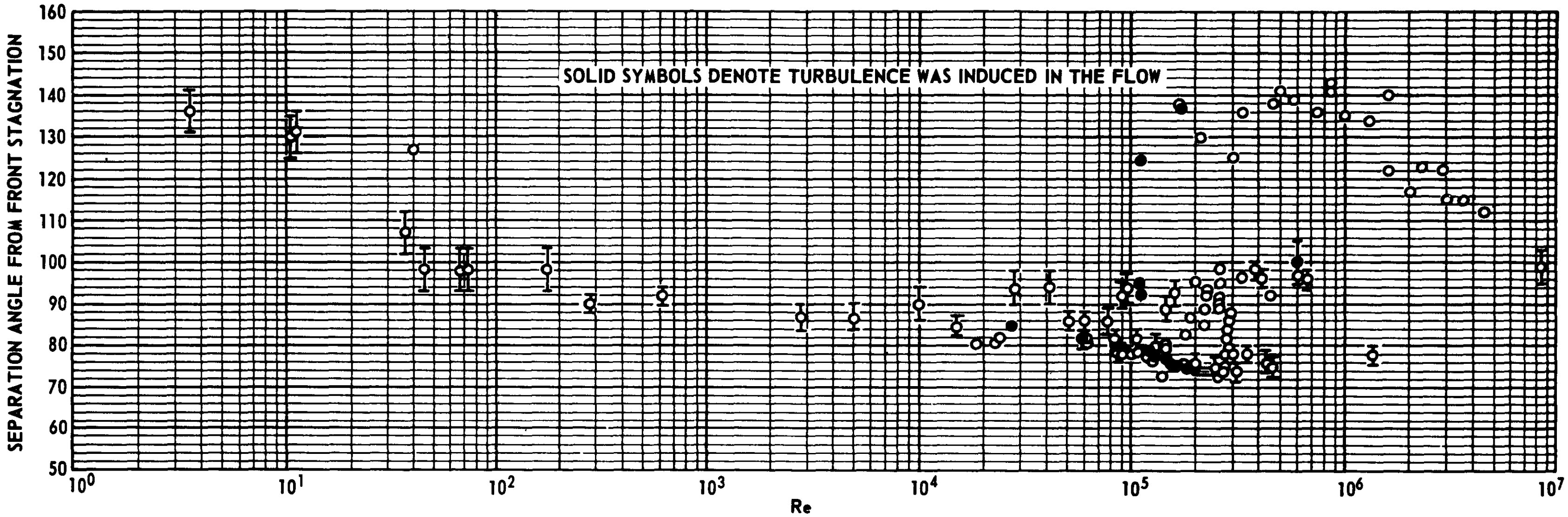

Figure 3 - Summary of All Experimental Data for Separation Angle versus Reynolds Number

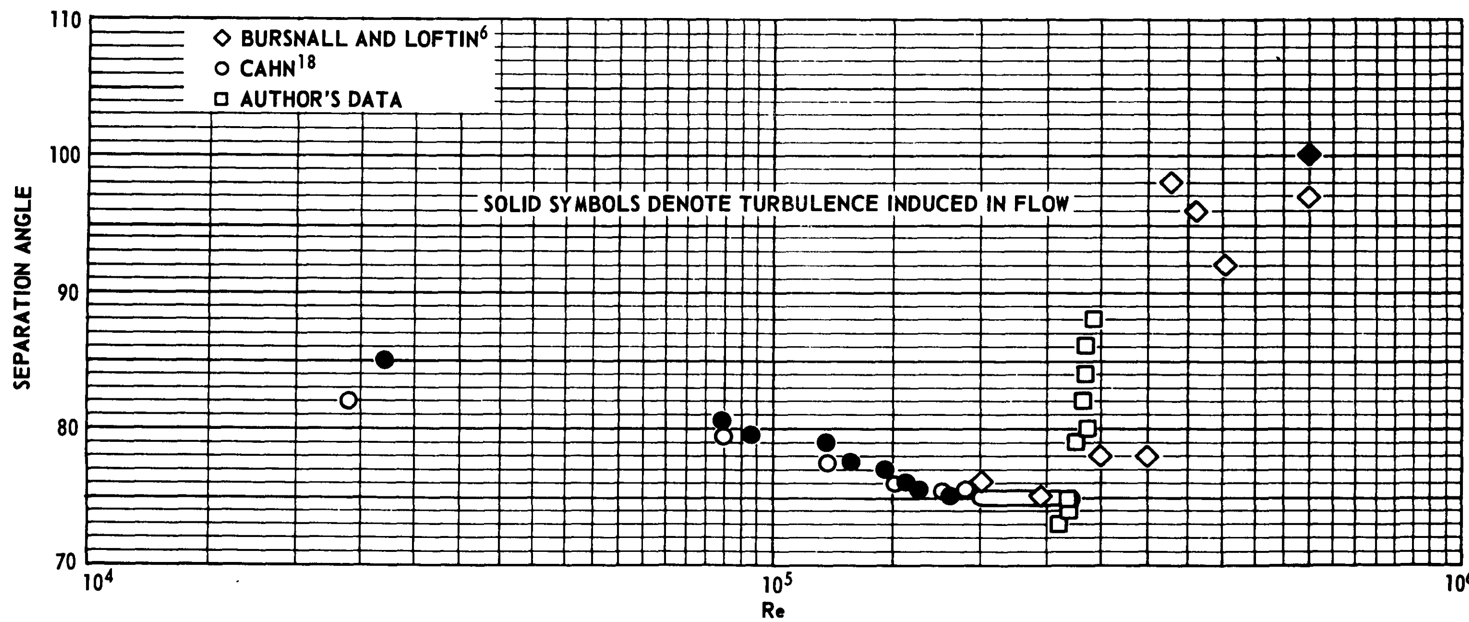

Figure 4 - Selected Data Showing Separation Angle versus Reynolds Number in the Transition Regime

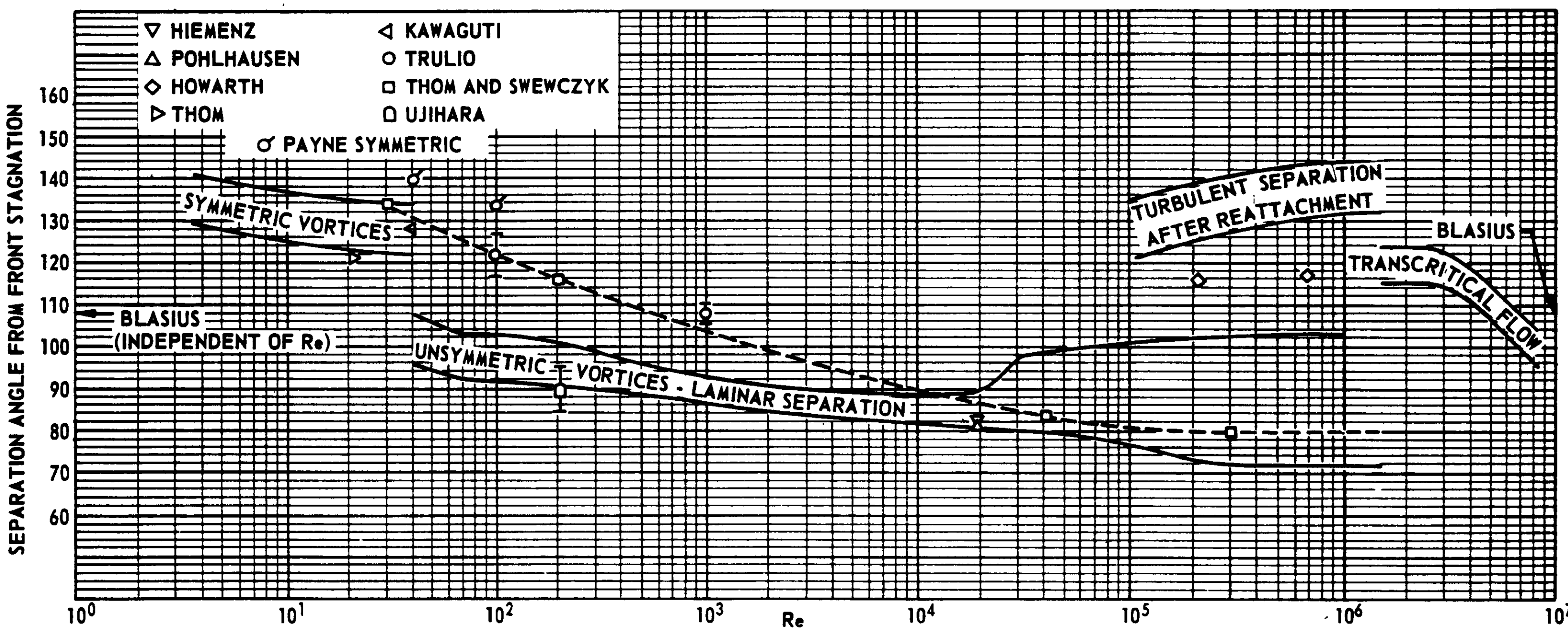

Figure 5 - Theoretical Results Compared with Experimental Results for Separation Angle versus Reynolds Number

TABLE 1

Summary of Experimental Results from Existing Literature

Investigator and Reference	Reynolds Number R_n	Separation Angle Θ_s	Mach Number M	Fluid Media	Induced Turbulence
RESULTS FROM PRESSURE DATA:					
Hiemenz[2]	1.85×10^4	81		Air	No
	2.25×10^4	81		Air	No
Fage and Falkner[3]	0.60×10^5	82 ± 2		Air	Yes
	0.60×10^5	82 ± 2		Air	No
	0.83×10^5	82 ± 2		Air	No
	1.06×10^5	82 ± 2		Air	No
Flachsbart[4]	6.7×10^5	96 ± 2		Air	No
	1.9×10^5	87 ± 1		Air	No
Thom[5]	3.5	136 ± 5		Oil	No
	11.2	131 ± 5		Oil	↓
	10.5	130 ± 5		Oil	↓
	36	107 ± 5		Oil	↓
	45	98 ± 5		Water	↓
	67	98 ± 5		Water	↓
	73	98 ± 5		Water	↓
	174	98 ± 5		Water	No
Bursall and Loftin[6]	2.00×10^5	76 ± 2			No
	2.45×10^5	75 ± 2			↓
	3.00×10^5	78 ± 2			↓
	3.50×10^5	78 ± 2			↓
	3.77×10^5	98 ± 2			↓
	4.07×10^5	96 ± 2			↓
	4.54×10^5	92 ± 1			↓
	5.96×10^5	97 ± 1			No
	5.96×10^5	100 ± 5			Yes
Fage[7]	3.3×10^5	96.4		Air	No
Gowen and Perkins[8]	3.14×10^5	74 ± 2	0.05	Air	No
	4.26×10^5	76 ± 2	0.06-0.07	↓	↓
	0.51×10^5	86 ± 2	0.3	↓	↓
	0.85×10^5	79 ± 2	0.3	↓	↓
	0.77×10^5	86 ± 3	0.5	↓	↓
	1.29×10^5	80 ± 3	0.5	↓	↓
	0.88×10^5	92 ± 3	0.6	↓	↓
	1.46×10^5	89 ± 3	0.6	↓	↓
	0.95×10^5	94 ± 3	0.7	↓	↓
	1.57×10^5	93 ± 3	0.7	Air	No
Roshko[9]	1.45×10^5	80 ± 1		Air	No
Roshko[10]	8.4×10^6	95 - 103		Air	No

Table 1 (Continued)

Investigator and Reference	Reynolds Number R_n	Separation Angle θ_s	Mach Number M	Fluid Media	Induced Turbulence
Schiller and Linke[11]	2800	87 ± 3			
	5000	87 ± 3			
	9900	90 ± 4			
	2.77×10^4	94 ± 4			
	4.07×10^4	94 ± 4			
Schwabe[12]	285	90 ± 2			
	625	92 ± 2			
Thom[13]	4.6×10^5	75 ± 2		Air	No
	1.35×10^6	78 ± 2		Air	No
RESULTS FROM FLOW VISUALIZATION:					
Mattingly[15]	1.5×10^4	83.2- 87.4 (fwd most) 90.0-103.6 (aft most)		Water	No
	6.0×10^4	85.1-88.4		Water	No
Taneda[16]	40	127		Water	No
RESULTS FROM SHEAR DATA:					
Fage and Falkner[3]	2.12×10^5	130		Air	No
	1.66×10^5	139		↓	No
	1.06×10^5	78.5		↓	No
	1.68×10^5	137		↓	Yes
	1.08×10^5	92.5, 95, 124.5		Air	Yes
Cahn[18]	2.7×10^4	85		Air	Yes
	8.4×10^4	80.5		↓	↓
	9.3×10^4	79.5		↓	↓
	1.2×10^5	79		↓	↓
	1.3×10^5	77.5		↓	↓
	1.45×10^6	77		↓	↓
	1.55×10^5	76		↓	↓
	1.65×10^5	75.5		↓	↓
	1.8×10^5	75		↓	Yes
	2.4×10^4	82		↓	No
	8.5×10^4	79.5		↓	↓
	1.2×10^5	77.5		↓	↓
	1.5×10^5	76		↓	↓
	1.75×10^5	75.5		↓	↓
	1.9×10^5	75.5		↓	↓
	$2.0\text{-}2.7 \times 10^5$	75 ± 0.5		Air	No

Table 1 (Continued)

Investigator and Reference	Reynolds Number R_n	Separation Angle θ_s	Mach Number M	Fluid Media	Induced Turbulence
Achenbach[17]	6×10^4	81	< 0.1	Air	No
	9×10^4	78			
	10^4	78			
	1.25×10^5	76			
	1.4×10^5	73			
	1.45×10^5	79			
	1.8×10^5	83			
	2.0×10^5	95			
	2.2×10^5 2.3×10^5	85, 89, 92, 94			
	2.6×10^5	89, 91, 92, 95, 98			
	3×10^5	125			
	3.3×10^5	136			
	4.6×10^5	138			
	5×10^5	141			
	5.8×10^5	139			
	7.4×10^5	136			
	8.6×10^5	141, 143			
	10^6	135			
	1.3×10^6	134			
	1.6×10^6	122, 140			
	2×10^6	117			
	2.3×10^6	123			
	2.9×10^6	122			
	3.0×10^6	115			
	3.6×10^6	115			
	4.5×10^6	112	< 0.1	Air	No

TABLE 2

Experimental Data of Author

Separation Angle ↓	Reynolds Numbers* $\times 10^{-5}$							
	Gage H3		Gage H5		Gage H10		Gage H11	
	U_∞↑	U_∞↓	U_∞↑	U_∞↓	U_∞↑	U_∞↓	U_∞↑	U_∞↓
72.6	2.79	2.47	2.79	2.47	2.79	2.60	2.79	2.62
74.3	3.01	2.60	3.01	2.60	2.94	2.70	2.94	2.70
75.1	2.96	2.53	2.94	2.53	3.21	2.70	3.21	2.79
76.0	2.87	--	2.87	--	3.18	--	3.18	--
78.0	2.63	2.50	2.63	2.50	2.94	2.74	2.94	2.74
78.0	2.79	--	2.79	--	2.80	--	2.80	--
80.0	3.17	2.45	3.17	2.45	3.17	2.87	3.17	2.87
82.0	3.11	2.62	3.11	2.62	2.87	2.82	2.87	2.82
83.9	3.01	2.67	3.01	2.67	3.04	2.84	3.04	2.84
86.0	3.07	2.79	3.07	2.79	2.91	2.84	2.91	2.84
88.0	3.21	2.62	3.21	2.87	2.97	2.94	2.97	2.94

*Fluid media = water, no induced turbulence.

TABLE 3

Summary of Theoretical Results

Reference	Reynolds Number R_n	Separation Angle Θ_s deg	Approach
Blasius[22]	Not specified	108.8	Boundary layer equations and potential flow pressure distribution (Power series to X^7)
Blasius[22]	Not specified	109.6	Boundary layer equations and potential flow pressure distribution (Power series to X^9)
Pohlhausen[31]	Not specified	109.5	Approximate Blasius boundary layer equations and potential flow pressure distribution
Hiemenz[2]	1.85×10^4	82	Blasius boundary layer equations and experimental pressure distribution
Pohlhausen[31]	1.85×10^4	81.5	Approximate Blasius boundary layer equations and experimental pressure distribution
Howarth[30]	2.12×10^5	116	Hiemenz solution
Howarth[30]	6.7×10^5	117	Hiemenz solution
Ujihara[31]	200	90 ± 5	Numerical solution using potential theory and generalized Kutta condition
Thom[5]	20	122	Numerical solution using steady vorticity equations
Kawaguti[33]	40	127.8	Numerical solution using steady vorticity equations
Payne[34]	40 100	140 134	Numerical solution using unsteady vorticity equations
Trulio et al.[35]	100 1000	122 ± 5 108 ± 2	Numerical solution using unsteady vorticity equations
Thoman and Szewczyk[36]	30 200 4×10^4 3×10^5	134 116 84 80	Numerical solution using unsteady vorticity equations

Table 1 (Continued)

Investigator and Reference	Reynolds Number R_n	Separation Angle θ_s	Mach Number M	Fluid Media	Induced Turbulence
Achenbach[17]	6×10^4	81	< 0.1	Air	No
	9×10^4	78			
	10^4	78			
	1.25×10^5	76			
	1.4×10^5	73			
	1.45×10^5	79			
	1.8×10^5	83			
	2.0×10^5	95			
	2.2×10^5 2.3×10^5	85, 89, 92, 94			
	2.6×10^5	89, 91, 92, 95, 98			
	3×10^5	125			
	3.3×10^5	136			
	4.6×10^5	138			
	5×10^5	141			
	5.8×10^5	139			
	7.4×10^5	136			
	8.6×10^5	141, 143			
	10^6	135			
	1.3×10^6	134			
	1.6×10^6	122, 140			
	2×10^6	117			
	2.3×10^6	123			
	2.9×10^6	122			
	3.0×10^6	115			
	3.6×10^6	115			
	4.5×10^6	112	< 0.1	Air	No

TABLE 2

Experimental Data of Author

Separation Angle ↓	Reynolds Numbers* $\times 10^{-5}$							
	Gage H3		Gage H5		Gage H10		Gage H11	
	U_∞↑	U_∞↓	U_∞↑	U_∞↓	U_∞↑	U_∞↓	U_∞↑	U_∞↓
72.6	2.79	2.47	2.79	2.47	2.79	2.60	2.79	2.62
74.3	3.01	2.60	3.01	2.60	2.94	2.70	2.94	2.70
75.1	2.96	2.53	2.94	2.53	3.21	2.70	3.21	2.79
76.0	2.87	--	2.87	--	3.18	--	3.18	--
78.0	2.63	2.50	2.63	2.50	2.94	2.74	2.94	2.74
78.0	2.79	--	2.79	--	2.80	--	2.80	--
80.0	3.17	2.45	3.17	2.45	3.17	2.87	3.17	2.87
82.0	3.11	2.62	3.11	2.62	2.87	2.82	2.87	2.82
83.9	3.01	2.67	3.01	2.67	3.04	2.84	3.04	2.84
86.0	3.07	2.79	3.07	2.79	2.91	2.84	2.91	2.84
88.0	3.21	2.62	3.21	2.87	2.97	2.94	2.97	2.94

*Fluid media = water, no induced turbulence.

16. Taneda, S., "Experimental Investigation of the Wake behind Cylinders and Plates at Low Reynolds Numbers," Research Institute for Applied Mechanics, Vol. IV, No. 14, pp. 29-40 (Oct 1955).

17. Achenbach, E., "Distribution of Local Pressure and Skin Friction around a Circular Cylinder in Cross-Flow up to $R_e = 5 \times 10^6$," J. Fluid Mech., Vol. 34 (Dec 1968).

18. Cahn, R. S., "The Nature of Flow Separation from a Circular Cylinder near the Critical Reynolds Number," Master's Thesis, University of Maryland (1963).

19. "Instructional Manual: Pitch-Heave Oscillator System," Consolidated Systems Corporation TM 3-3081 (15 Apr 1964).

20. Lamb, H., "Hydrodynamics," First American Edition, Dover Publications, New York (1945).

21. Schlichting, H., "Boundary Layer Theory," McGraw-Hill, New York (1955).

22. Blasius, H., "Grenzschichten in Flüssigkeiten mit kleiner Reibung," Z. Math. u. Phys., Vol. 56, No. 1 (1908); English Translation NACA TM 1256.

23. Thwaites, B., "Approximate Calculation of the Laminar Boundary Layer," Aeronautical Quarterly, Vol. I, p. 245 (Nov 1949).

24. Stratford, B. S., "Flow in the Laminar Boundary Layer near Separation," ARC R&M 3002 (Nov 1954).

25. Tani, I., "On the Approximate Solution of the Laminar Boundary-Layer Equations," J. of Aero. Sci., Vol. 21 (Jul 1954).

26. Curle, N. and Skan, S. W., "Approximate Methods for Predicting Separation Properties of Laminar Boundary Layers," Aeronautical Quarterly, Vol. VIII, p. 257 (Aug 1957).

27. Smith, A. M. O. and Clutter, D., "Solution of the Incompressible Laminar Boundary Layer Equations," Douglas Aircraft Company Report ES 40445 (Jul 1961).

28. Meksyn, D., "New Methods in Laminar Boundary-Layer Theory," Pergamon Press, New York (1961).

29. Terrill, R., "Approximate Methods for Solving the Laminar Boundary-Layer Equations," Aeronautical Quarterly (Aug 1962).

30. Howarth, L., Proc. Camb. Phil. Soc., Vol. 31, pp. 585-588 (1935).

31. Pohlhausen, K., "Zur näherungsweisen Integration der Differentialglechung der laminaren Reibungsschicht," ZAMM, Vol. 1, pp. 252-268 (1921).

32. Ujihara, B. H., "An Analytical Study of Separated Flow about a Circular Cylinder," NAA S&ID, SID 65-1730 (Jan 1966).

33. Kawaguti, M., "Numerical Solution of the Navier-Stokes Equation for the Flow Around a Circular Cylinder at Reynolds Number 40," J. Phys. Soc. of Japan, Vol. 8, No. 6, pp. 747-757 (1953).

34. Payne, R. B., "Calculations of Unsteady Viscous Flow Past a Circular Cylinder," J. Fluid Mech., Vol. 4, Part 1, pp. 81-86 (May 1958).

35. Trulio, J. G. et al., "Calculation of Two-Dimensional Turbulent Flow Fields," NASA CR-430 (May 1966).

36. Thoman, D. C. and Szewczyk, A. A., "Numerical Solutions of Time Dependent Two Dimensional Flow of a Viscous, Incompressible Fluid over Stationary and Rotating Cylinders," University of Notre Dame Technical Report 66-14 (Jul 1966).

INITIAL DISTRIBUTION

Copies	
1	CNO Attn: OP 098T6 Henry Cheng
1	CHNAVMAT (MAT 0331)
7	NAVSHIPSYSCOM 1 SHIPS 0342 1 SHIPS 037 3 SHIPS 2052 1 PMS 381 1 SHIPS 03412
12	DDC
1	ONR Attn: Mr. Ralph D. Cooper Code 438
1	ONR, Boston
1	ONR, Chicago
1	ONR, New York
1	ONR, Pasadena
1	ONR, San Francisco
5	NRL 3 Library, Code 2029 1 Mr. Charles Votaw 1 Dr. G. H. Koopman
1	NAVFACENGCOMHQ Attn: Code 0321
7	NAVSEC 1 SEC 6110 1 SEC 6114D 1 SEC 6136 1 SEC 6140 1 SEC 6144G 1 SEC 6034B 1 SEC 6053B
2	NAVAIRDEVCEN 1 Technical Library 1 Mr. J. R. Dale
1	NAVUSEARANDCEN PASADENA Attn: Dr. J. Hoyt
1	NURDC, San Diego Attn: Dr. A. Fabula

Copies	
1	NELC Attn: Library
1	NRL (Code 2027)
1	NUSC NPT
1	NWL Attn: Technical Library
1	CIVENGRLAB Attn: Code L31
1	NAVWPNSCEN Attn: Code 753
1	NAVSHIPYD BSN Attn: Technical Library
1	NAVSHIPYD CHASN Attn: Technical Library
1	NAVSHIPYD NORVA Attn: Technical Library
1	NAVSHIPYD HUNTERS PT Attn: Technical Library
1	NAVSHIPYD PEARL Attn: Code 246-P
1	NAVSHIPYD PHILA Attn: Code 240
1	NAVSHIPYD PTSMH Attn: Technical Library
1	NAVSHIPYD BREM Attn: Engr Library
3	NAVSHIPYD MARE ISLAND 1 Technical Library 1 Code 250 1 Code 130L1
1	AFFDL (FDDS-Mr. J. Olsen) Wright-Patterson AFB, Dayton, Ohio 45433
1	NASA Scientific and Technical Information Facility P. O. Box 33 College Park, Md. 20740

Copies

1 AFORSR (SREM)
1400 Wilson Blvd.
Arlington, Va. 22209

2 COMDTCOGARD
1 Div Merchant Marine Safety
1 Sta 5-2

1 BUSTAND
Attn: P. S. Klebanoff,
Fluid Mech Br

1 Dir of Res, NASA
600 Independence Ave., S. W.
Wash., D. C. 20546

1 Director
Waterways Experiment Station
Box 631
Vicksburg, Miss. 39180
Attn: Res Center Library

1 NAVORD (Code ORD-035)

1 Library of Congress
Science and Tech Div
Wash., D. C. 20540

1 Univ of Bridgeport
Bridgeport, Conn. 06602
Attn: Prof. Earl Uram
Mech Engr Dept

1 Brown Univ
Providence, R.I. 02912
Attn: Div of Appl Math

4 Naval Architecture Dept
College of Engr
Univ of California
Berkeley, Calif. 94720
1 Librarian
1 Prof. J. R. Paulling
1 Prof. J. V. Wehausen
1 Dr. H. A. Schade

3 California Inst of Tech
Pasadena, Calif. 91109
1 Dr. A. J. Acosta
1 Dr. T. Y. Wu
1 Dr. M. S. Plesset

1 Univ of Connecticut
Box U-37,
Storrs, Conn. 06268
Attn: Prof. V. Scottorn
Hydr Res Lab

Copies

1 Cornell Univ
Grad Sch of Aerospace Engr
Ithaca, N. Y. 14850
Attn: Prof. W. R. Sears

1 Harvard Univ
2 Divinity Ave
Cambridge, Mass. 02138
Attn: Prof. G. Birkhoff
Dept of Math

1 Pierce Hall
Harvard Univ
Cambridge, Mass. 02138
Attn: Prof. G. F. Carrier

1 Univ of Illinois
College of Engr
Urbana, Ill. 61801
Attn: Dr. J. M. Robertson
Theoretical & Applied
Mechanics Dept

1 The Univ of Iowa
Iowa City, Iowa 52240
Attn: Dr. Hunter Rouse

1 The Univ of Iowa
Iowa Inst of Hydraulic Res
Iowa City, Iowa 52240
Attn: Dr. J. Kennedy

1 The Johns Hopkins Univ
Mechanics Dept
Baltimore, Md. 21218
Attn: Prof. O. M. Phillips

1 Kansas State Univ
Engineering Experiment Station
Seaton Hall
Manhattan, Kansas 66502
Attn: Prof. D. A. Nesmith

1 Univ of Kansas
Lawrence, Kansas 60644
Attn: Chm Civil Engr Dept

1 Lehigh Univ
Bethlehem, Penna. 18015
Attn: Fritz Lab Library

1 Long Island Univ
Grad Dept of Marine Science
40 Merrick Ave
East Meadow, N. Y. 11554
Attn: Prof. David Price

Copies

3 Univ of Maryland
Mech Engr Dept
College Park, Md.
1 Dr. C. L. Sayre
1 Dr. J. E. John
1 Dr. F. Buckley

1 MIT, Hydrodynamics Lab
Cambridge, Mass. 02139
Attn: Prof. A. T. Ippen

7 MIT, Dept of Naval Arch and Marine Engr
Cambridge, Mass. 02139
1 Dr. A. H. Keil
1 Prof. P. Mandel
1 Prof. J. R. Kerwin
1 Prof. P. Leehey
1 Prof. M. Abkowitz
1 Prof. F. M. Lewis
1 Dr. J. N. Newman

3 Univ of Michigan
Dept of Naval Arch and Marine Engr
Ann Arbor, Mich. 48104
1 Dr. T. F. Ogilvie
1 Prof. H. Benford
1 Dr. F. C. Michelsen

5 St. Anthony Falls Hydraulic Lab
Univ of Minnesota
Miss. River at 3rd Ave., S.E.
Minneapolis, Minn. 55414
1 Director
1 Dr. C. S. Song
1 Mr. J. M. Killeen
1 Mr. F. Schiebe
1 Mr. J. M. Wetzel

3 U. S. Naval Academy
Annapolis, Md. 21402
1 Library
1 Dr. Bruce Johnson
1 Prof. P. Van Mater

3 U. S. Naval Postgraduate Sch
Monterey, Calif. 93940
1 Library
1 Prof. J. Miller
1 Dr. T. Sarpkaya

Copies

1 Newark Univ
College of Engr
323 High St.
Newark, N. J. 07102
Attn: Dr. W. L. Haberman

1 New York Univ
University Heights
Bronx, N. Y. 10453
Attn: Prof. W. Pierson, Jr.

2 New York Univ
Courant Inst of Math Sci
251 Mercier Street
New York, N. Y. 10012
1 Prof. A. S. Peters
1 Prof. J. J. Stoker

3 Univ of Notre Dame
Notre Dame, Ind. 46556
1 Dr. A. Strandhagen
1 Dr. J. Nicolaides
1 Prof. A. A. Szewczyk

1 Ohio Northern Univ
College of Engr
Ada, Ohio
Attn: Dr. R. J. Glass

1 The Pennsylvania State Univ
Ordnance Res Lab
University Park, Penna. 16801
Attn: Director

1 Colorado State Univ
Dept of Civil Engr
Fort Collins, Colo. 80521
Attn: Prof. M. Albertson

1 Aerodynamics Lab
Dept of Aerospace and Mech Sci
The James Forrestal Res Center
Princeton Univ
Attn: Prof. G. Mellor

1 Scripps Inst of Oceanography
Univ of California
LaJolla, Calif. 92038
Attn: J. Pollock

3 Stanford Univ
Stanford, Calif. 94305
1 Prof. H. Ashley, Dept of Aero and Astro
1 Prof. R. Street
1 Prof. B. Perry, Dept Civ Engr

Copies	
3	Stevens Inst of Tech Davidson Lab 711 Hudson Street Hoboken, N. J. 07030 1 Dr. J. P. Breslin 1 Dr. S. Tsakonas 1 Library
1	Univ of Texas Defense Res Lab P. O. Box 8029 Austin, Texas 78712 Attn: Director
1	Univ of Washington Appl Phys Lab 1013 N. E. 40th St. Seattle, Wash. 98105 Attn: Director
2	Webb Inst of Nav Arch Crescent Beach Road Glen Cove, L.I., N.Y. 11542 1 Prof. E. V. Lewis 1 Prof. L. W. Ward
1	Worcester Polytechnic Inst Alden Res Laboratories Worcester, Mass. 01609 Attn: Director
1	Aerojet-General Corp 1100 W. Hollyvale St. Azusa, Calif. 91702 Attn: Mr. J. Levy, Bldg 160, Dept 4223
1	Bethlehem Steel Corp Central Technical Div Sparrows Point Yard Sparrows Point, Md. 21219 Attn: Mr. A. Haff, Tech Mgr
1	Bolt Beranek & Newman, Inc 1501 Wilson Blvd Arlington, Va. 22209 Attn: Dr. F. Jackson
1	Cornell Aeronautical Lab Appl Mech Dept P. O. Box 235 Buffalo, N. Y. 14221

Copies	
1	Electric Boat Div General Dynamics Corp Groton, Conn. 06340 Attn: Mr. V. Boatwright, Jr.
1	Esso International 15 West 51st Street New York, N. Y. 10019 Attn: Mr. R. J. Taylor, Mgr R & D Tanker Dept
1	General Appli Sci Lab Inc Merrick & Stewart Avenues Westbury, L.I., N.Y. 11590 Attn: Dr. F. Lane
1	Gibbs & Cox, Inc. 21 West Street New York, N. Y. 10006 Attn: Tech Libr
1	Grumman Aircraft Engineering Corp Bethpage, L.I., N.Y. 11714 Attn: Mr. W. Carl
2	Hydronautics, Inc. Pindell School Road Howard County Laurel, Maryland 20810 1 Mr. P. Eisenberg 1 Mr. M. Tulin
2	McDonnell Douglas Aircraft Co Douglas Aircraft Div 3855 Lakewood Blvd Long Beach, Calif. 90801 1 Mr. John Hess 1 Mr. A. M. O. Smith
1	Measurement Analysis Corp 10960 Santa Monica Blvd Los Angeles, Calif. 90025
1	National Science Foundation Engineering Division 1800 G St., N. W. Wash., D. C. 20550 Attn: Director
1	Newport News Shipbuilding and Dry Dock Company 4101 Washington Ave Newport News, Va. 23607 Attn: Tech Libr Dept

Copies	
1	Oceanics, Incorporated Technical Industrial Park Plainview, L.I., N.Y. 11803 Attn: Dr. Paul Kaplan
1	Robert Taggart, Inc. 3930 Walnut Street Fairfax, Va. 22030 Attn: Mr. R. Taggart
1	Society of Naval Architects and Marine Engineers 74 Trinity Place New York, N. Y. 10006
2	Southwest Res Inst 8500 Culebra Road San Antonio, Tex. 78206 1 Dr. H. Abramson 1 Appl Mech Review
1	Tracor, Incorporated 6500 Tracor Lane Austin, Tex. 78721
1	Eastern Research Group P. O. Box 222 Church Street Station New York, N. Y. 10008
1	Naval Ship Engineering Center Norfolk Division Boat Engineering Dept Norfolk, Va. 28511 Attn: Mr. D. L. Blount, Code 6660

Copies	
1	Woods Hole Oceanographic Inst Woods Hole, Mass. 02543 Attn: Reference Room
1	Prof. Jerome Lurye Dept of Mathematics St. John's Univ Jamaica, N. Y. 11432
1	Mr. B. H. Ujihara North American Rockwell Inc. Space and Information Sys Div 12214 Lakewood Blvd Downey, Calif. 90241
1	Stanford Research Institute Menlo Park, Calif. 94025 Attn: Library
1	Cambridge Acoustical Associates, Inc. 129 Mount Auburn Street Cambridge, Mass. 02138 Attn: Mr. M. C. Junger
1	Dr. Roland W. Jeppson College of Engineering Utah State Univ Logan, Utah 84321
1	Dr. Albert T. Ellis Dept of Applied Mechanics Univ of Calif at San Diego P. O. Box 109 LaJolla, Calif. 92038

CENTER DISTRIBUTION

Copies	Code	
1	15	Dr. Cummings
1	154	Dr. Morgan
1	1541	
1	1544	
1	1548	
1	1552	
16	1556 15 D. W. Coder 1 D. S. Cieslowski	

Copies	Code
1	1564
1	1843
1	1942
1	1962
1	1966

UNCLASSIFIED

Security Classification

DOCUMENT CONTROL DATA - R & D

(Security classification of title, body of abstract and indexing annotation must be entered when the overall report is classified)

1. ORIGINATING ACTIVITY *(Corporate author)* Naval Ship Research and Development Center Bethesda, Maryland 20034	2a. REPORT SECURITY CLASSIFICATION UNCLASSIFIED 2b. GROUP

3. REPORT TITLE

LOCATION OF SEPARATION ON A CIRCULAR CYLINDER IN CROSSFLOW AS A FUNCTION OF REYNOLDS NUMBER

4. DESCRIPTIVE NOTES *(Type of report and inclusive dates)*

5. AUTHOR(S) *(First name, middle initial, last name)*

David W. Coder

6. REPORT DATE	7a. TOTAL NO. OF PAGES	7b. NO. OF REFS
November 1971	32	36

8a. CONTRACT OR GRANT NO b. PROJECT NO. Subproject S4611 010 c. Task 11098 d.	9a. ORIGINATOR'S REPORT NUMBER(S) 3647 9b. OTHER REPORT NO(S) *(Any other numbers that may be assigned this report)*

10. DISTRIBUTION STATEMENT

APPROVED FOR PUBLIC RELEASE: DISTRIBUTION UNLIMITED

11. SUPPLEMENTARY NOTES	12. SPONSORING MILITARY ACTIVITY
	Naval Ship Systems Command Washington, D. C.

13. ABSTRACT

All available information on the location of separation on a circular cylinder in crossflow as a function of Reynolds number (from "creeping" flow to "transcritical" flow) has been summarized. The results of an experiment by the author in the "transition" (or "supercritical") flow regime are included. The various theoretical and experimental results are discussed and compared. Areas needing additional theoretical and experimental work are pointed out.

DD FORM 1 NOV 65 1473 (PAGE 1)

S/N 0101-807-6801

UNCLASSIFIED

Security Classification

UNCLASSIFIED
Security Classification

14 KEY WORDS	LINK A		LINK B		LINK C	
	ROLE	WT	ROLE	WT	ROLE	WT
Separation						
Circular Cylinder						
Viscous Flow						
Turbulent Flow						
Vortex Shedding						

DD FORM 1 NOV 65 1473 (BACK)
(PAGE 2)

UNCLASSIFIED
Security Classification